SURFACE MATERIAL CLASSIFICATION BASED ON SPECTRAL SHAPE

M. J. Carlotto and V.T. Tom
The Analytic Sciences Corporation
One Jacob Way, Reading, Massachusetts

Since the feasibility of automatic pattern classification techniques in remote sensing applications was demonstrated in the mid 1960s, a variety of specialized techniques for surface material classification and related applications have been developed. Most of the techniques are based on statistical methods which use probability models to describe the spectral, spatial or temporal properties of material [2]. Recently, the use of heuristic methods for classifying surface materials in multispectral imagery has been proposed [1]. The essence of this approach is to describe surface material classes (SMCs) in terms of the relative intensities between bands (i.e., analysis of the spectral shape) and within bands (histogram analysis [3]). Potential advantages of such an approach are including provisions in a system for directly incorporating expert knowledge into the classifier (e.g., how a particular material ought to appear in a given image), for organizing the knowledge needed to recognize SMCs into explicit decision rules, and for extending the usefulness of the classifier to a wider range of scenes and imaging conditions [5].

In this paper a method for classifying SMCs based on the shape of the spectral signature is presented. Spectral shape is described in terms of a vector of predicates which specify the relative intensities between all pairs of bands. Spectral signatures are represented as logical expressions of shape predicates which define the classification logic. Preliminary results for Landsat TM image classification are discussed.

1. Spectral Shape Representation

Let the spectral measurement vector at pixel (i,j) be denoted $\underline{x}(i,j)$. We treat each spectral measurement $\underline{x} = \{x_n\}$ as an approximation to the spectrum at (i,j) where x_n is the spectral response in the n^{th} band. The goal of the present effort is to represent the spectral signature of SMCs by the shape of the spectrum instead of as points in the N-dimensional measurement space [7]. To illustrate this idea, consider the spectral plots in Fig. 1 from a four band sensor such as the Landsat MSS. The reflectivity of vegetation increases in the near IR while water is characterized as having a fairly low reflectivity in the visible and IR. In terms of the shape of their signatures, vegetation (a) is characterized as having a generally increasing response while water (f) has a decreasing one.

The proposed shape description is based on a specification of the relative intensities between all pairs of spectral bands. The resulting description is represented in the form of a conjunctive normal form expression (logical product) of binary variables or predicates $\underline{e} = \{p_{nm}\}$ where

$$p_{nm} = \begin{cases} 1 \text{ (true) if } x_n > x_m \\ 0 \text{ (false) otherwise} \end{cases} \quad (1)$$

For each spectral measurement, a logical expression or vector of predicates can be derived which contains $M = N(N-1)/2$ unique terms. By this method water and vegetation would be represented by the expressions

$$\underline{e}_{water} = \{ p_{12}\, p_{13}\, p_{14}\, p_{23}\, p_{24}\, p_{34} \} \quad (2a)$$

and

$$\underline{e}_{vegetation} = \{ p_{12}\, p_{31}\, p_{41}\, p_{32}\, p_{42}\, p_{43} \} \quad (2b)$$

Since if p_{nm} is true p_{mn} is false, only true predicates are indicated for notational convienence.

The above shape representation is a many to one transformation from the 2^{BN} state spectral measurement space to a 2^{M} state binary shape space where B is the number of bits. Shape space can be depicted graphically using Karnaugh maps [6] where each position in the K-map corresponds to a spectral shape. Typical signatures for vegetation and water are shown along with four other spectral shapes in Fig. 1. Their corresponding positions in shape space are shown in the K-map in Fig. 2. K-maps are arranged so that the Hamming distance (indicated in the upper left corner in the square) between nearest neighbors is equal to one. (The Hamming distance between two binary vectors of equal length is the number of bit positions which are different). The distances indicated in Fig. 2 are measured relative to the spectral shape (a) in Fig. 1. The above suggests use of the Hamming distance between spectral shape vectors as a natural measure of their similarity.

By using a binary representation, an expression for a class of spectral shapes $E(k)$ can be derived by simply "OR-ing" the $\underline{e}(i,j)$ shape vectors computed within the training region for that class. Fig. 3 shows two regions in a K-map which correspond to two hypothetical spectral shape classes defined by the logical expressions

$$\begin{aligned} E(1) &= \{ p_{21}\, p_{31}\, p_{41}\, p_{23}\, p_{42}\, p_{43} \} + \{ p_{21}\, p_{13}\, p_{41}\, p_{23}\, p_{42}\, p_{43} \} + \\ &\quad \{ p_{12}\, p_{13}\, p_{41}\, p_{23}\, p_{42}\, p_{43} \} + \{ p_{12}\, p_{31}\, p_{41}\, p_{23}\, p_{42}\, p_{43} \} \\ &= \{ p_{41}\, p_{23}\, p_{42}\, p_{43} \} \quad (3a) \\ E(2) &= \{ p_{21}\, p_{13}\, p_{41}\, p_{32}\, p_{42}\, p_{43} \} + \{ p_{21}\, p_{13}\, p_{41}\, p_{23}\, p_{42}\, p_{43} \} + \\ &\quad \{ p_{21}\, p_{13}\, p_{14}\, p_{23}\, p_{42}\, p_{43} \} + \{ p_{21}\, p_{13}\, p_{14}\, p_{32}\, p_{42}\, p_{43} \} \\ &= \{ p_{21}\, p_{13}\, p_{42}\, p_{43} \}. \quad (3b) \end{aligned}$$

The shaded areas define decision regions in shape space. Since $E(1)$ and $E(2)$ share the common term $\{ p_{21}\, p_{13}\, p_{41}\, p_{23}\, p_{42}\, p_{43} \}$, the two classes overlap as shown by the cross-hatched area in Fig. 3. Spectral shapes which fall in overlapping areas may be misclassified as discussed below.

2. Spectral Shape Classification

This section describes a decision logic classifier based on the spectral shape representation described in the previous section. The classifier shown in Fig. 4 consists of a comparator bank which computes the shape vector $\underline{e}(i,j)$ at each pixel in the image, a decision logic generator which deduces the logical expressions which define each spectral shape class from examples provided during training, and decision logic which assigns a class to each pixel in the image.

The decision logic generator deduces a logical expression $E(k)$ for each class of spectral signatures introduced. Using a procedure for learning conjunctive normal form expressions [9], $E(k)$ is initially set to the product of all possible band combination terms or predicates, e.g., for N=4

$$E(k) = \{ p_{12}\, p_{21}\, p_{13}\, p_{31}\, p_{14}\, p_{41}\, p_{23}\, p_{32}\, p_{24}\, p_{42}\, p_{34}\, p_{43} \}. \qquad (4)$$

For each spectral measurement within the training region for class k, all band pair combinations are examined. If the relation $x_n > x_m$ is observed, the predicate p_{mn} is deleted from $E(k)$. In the example in Fig. 3, for class 1, the terms

$$\{ p_{12}\, p_{13}\, p_{14}\, p_{32}\, p_{24}\, p_{34}\, p_{31}\, p_{21} \}$$

are deleted from $E(1)$. The resultant logic expression is equal to (3a). Repeating this procedure for each training set produces the set of logical expressions $\{E(k)\}$ which define the classification logic.

During classification the decision logic evaluates each of the E(k) expression and assigns classes to pixels. For example, $E(1)$ defines the decision rule

$$If : (x_4 > x_1) \text{ and } (x_2 > x_3) \text{ and } (x_4 > x_2) \text{ and } (x_4 > x_3)$$

$$Then : Assign\ y_1\ to\ y(i,j)$$

where y_1 is the label for class 1. Due to potential overlap betwween classes, i.e., if the decision regions overlap as shown in Fig. 3, multiple $E(k)$ may be true. Alternatively, if the $E(k)$ do not completely fill the K-map, then no $E(k)$ may be true and no class assigned in some cases. The latter may be regarded as desirable since one may not want to classify pixels whose spectral shape does not match any known signature. Otherwise, pixels can be assigned to the nearest class based on the Hamming distance.

Resolving the conflict of more than one $E(k)$ being true may be handled in several ways. For example, one could select the class whose logical expression or decision rule contains the greatest number of terms, or alternatively, the fewest number of "don't cares". Another possibility is to choose the class based on spatial considerations such as context [8]. Still another method is to use the characteristics error method [4]. In our initial experiments the $E(k)$ are evaluated sequentially so the class assignment is made according to which expression first evaluates true.

3. Discussion

The above use of four band data such as Landsat MSS serves to illustrate the key points of the technique. Current interest is in applying the technique to sensors with a greater number of bands (e.g., Landsat TM). In initial experiments on Landsat TM imagery, we are using the technique for classifying general land cover classes such as water, forest, dense and sparse vegetation, plowed fields, concrete and asphalt. Relative to the training set, a classification accuracy of 88% was achieved. This compared to an accuracy of 71% for a minimum distance classifier over the same area. While these results are not significant in themselves, the fact that the shape classifier tended to confuse related SMCs, i.e., those with similar spectral shapes such as sparse and dense vegetation while the minimum-distance classifier confused unrelated SMCs such as water and asphalt is worth noting.

On going work involves further testing the technique on additional Landsat TM data sets. Future plans include incorporating the technique within our Multispectral Image Analysis System [5], and investigating extensions of the method to multi-temporal data for vegetation classification.

References

[1] M.J. Carlotto, V.T. Tom, P.W. Baim and R.A. Upton, "Knowledge-based multispectral image classification", *Proceedings SPIE*, Vol. 504, 1984, San Diego, CA.

[2] M.J. Carlotto, "Techniques for multispectral image classification", *Proceedings SPIE*, Vol. 528, 1984, Los Angeles, CA.

[3] M.J. Carlotto, "Histogram analysis using a scale-space approach", *Proceedings from 1985 Computer Vision and Pattern Recognition Conference*, San Francisco, CA.

[4] R.D. Ferrante, "The characteristic error approach to conflict resolution", *1985 International Joint Conference on Artificial Intelligence*, Los Angeles, CA.

[5] R.D. Ferrante, M.J. Carlotto, J.M. Pomarede and P.W. Baim, "Multispectral image analysis system", *First Conference on Artificial Intelligence Applications*, December 1984, Denver, Colorado.

[6] F.J. Hill and G.R. Peterson, *Introduction to Switching Theory and Logical Design*, Wiley, 1974.

[7] P.H. Swain, "Fundamentals of pattern recognition in remote sensing," in *Remote Sensing: The Quantitative Approach*, McGraw Hill, 1978.

[8] J.C. Tilton and P.H. Swain, "Contextual classification of multispectral image data", *IGARSS*, June 1981, Washington, D.C.

[9] L.G. Valiant, "A theory of the learnable," *Communications of the ACM*, Vol. 27, No. 11, November 1984.

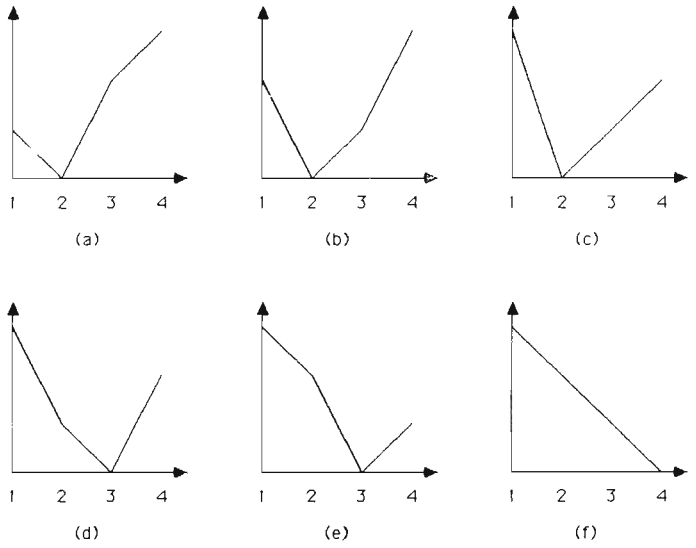

Fig. 1 Plots of spectral measurement vectors (relative intensity vs. spectral band)

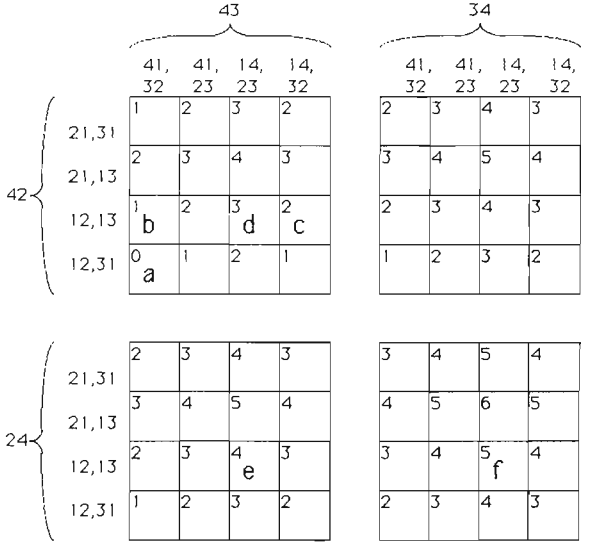

Fig. 2 K-map representation of spectral shape

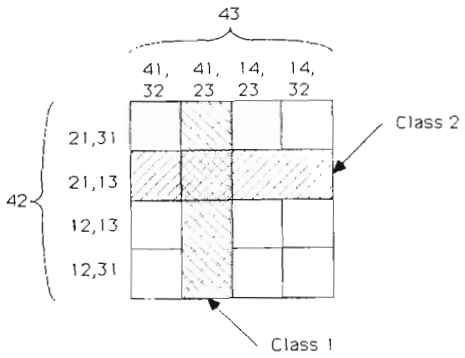

Fig. 3 Decision regions in K-map for shape classification

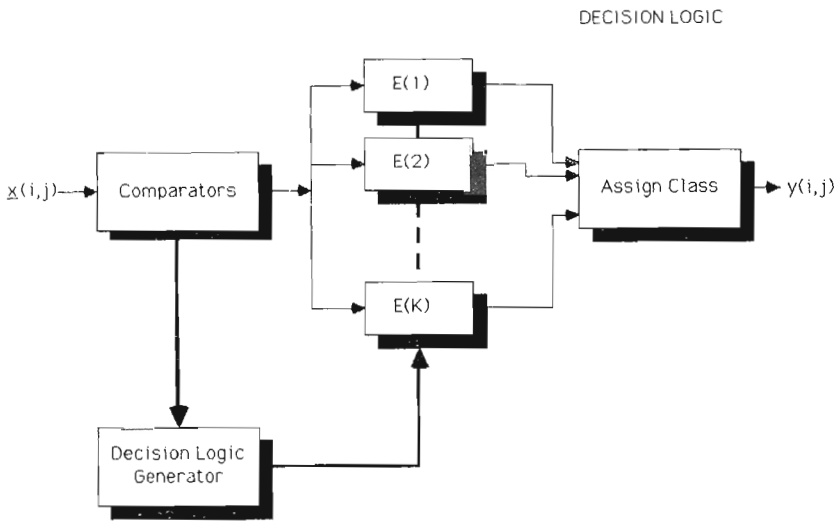

Fig. 4 Block diagram of decision logic for spectral shape classification